

# Relativistic Force-Free Electrodynamic Simulations of Neutron Star Magnetospheres

Jonathan C. McKinney<sup>\*</sup>

*Institute for Theory and Computation, Harvard-Smithsonian Center for Astrophysics, 60 Garden Street, MS 51, Cambridge, MA 02138, USA*

Accepted 2006 January 18. Received 2006 January 17; in original form 2005 December 8

## ABSTRACT

The luminosity and structure of neutron star magnetospheres are crucial to our understanding of pulsar and plerion emission. A solution found using the force-free approximation would be an interesting standard with which any model with more physics could be compared. Prior quasi-analytic force-free solutions may not be stable, while prior time-dependent magnetohydrodynamic models used unphysical model parameters. We use a time-dependent relativistic force-free electrodynamics code with no free parameters to find a unique stationary solution for the axisymmetric rotating pulsar magnetosphere in a Minkowski space-time in the case of no surface currents on the star. The solution is similar to the force-free quasi-analytic solution of Contopoulos et al. (1999) and the numerical magnetohydrodynamic solution of Komissarov (2005). The magnetosphere structure and the usefulness of the classical y-point in the general dissipative regime are discussed. The pulsar luminosity is found to be  $L \approx 0.99 \pm 0.01 \mu^2 \Omega_\star^4 / c^3$  for dipole moment  $\mu$  and angular frequency  $\Omega_\star$ .

**Key words:** stars:pulsars:general – stars:winds and outflows – relativity – force-free

## 1 INTRODUCTION

Neutron star magnetospheres are suspected to have large regions of space that are nearly force-free (Goldreich & Julian 1969; Ruderman & Sutherland 1975). Self-consistent quasi-analytic solutions exist that describe the force-free (and some magnetohydrodynamic (MHD)) parts of the environment of such systems (see, e.g., Contopoulos et al. 1999; Goodwin et al. 2004; Gruzinov 2005). Quasi-analytic methods cannot test the stability of their solutions and there is little hope to study the general nonaligned rotator.

Recently, Komissarov (2005) used a time-dependent numerical code to directly integrate the force-free and MHD equations of motion. They considered their force-free solution unphysical due to uncontrolled fast reconnection in the current sheet that led to closed field lines far beyond the light cylinder. Their MHD version had no such defect, but they were forced to introduce unphysical evolution equations and parameters (see their section 4.2) in order to avoid numerical errors and strong unphysical features. They found a stationary MHD solution that may be unique, but they were uncertain whether their solution depended upon the unphysical model parameters.

We investigate axisymmetric neutron star magnetospheres by integrating the force-free equations of motion

using a newly developed general relativistic force-free electrodynamics (GRFFE) extension (McKinney 2005d) to a general relativistic magnetohydrodynamics (GRMHD) code called HARM (Gammie et al. 2003). The original GRMHD code has been successfully used to study GRMHD models of accretion flows, winds, and jets (Gammie et al. 2003; Gammie, Shapiro, & McKinney 2004; McKinney & Gammie 2004; McKinney 2005a,b,c). The GRFFE formulation is a simple extension of HARM, so all the code developed for HARM is immediately useful and has identical convergence properties to the GRMHD version. We have shown that our GRFFE formulation is at least as accurate as the GRFFE formulation by Komissarov (2002, 2004) (McKinney 2005d). Parabolic spatial interpolation and fourth-order Runge-Kutta temporal integration are used to improve accuracy. Compared to Komissarov (2005), our force-free scheme is improved by significantly lowering the reconnection rate in current sheets by forcing numerically induced velocities into current sheets to vanish. This eliminates all the difficulties encountered by Komissarov (2005).

Section 2 discusses the solution of the neutron star magnetosphere. Section 3 summarizes the results of the paper. The notation follows Misner et al. (1973) and the signature of the metric is  $-+++$ . Tensor components are given in a coordinate basis. The components of the tensors of interest are given by  $F^{\mu\nu}$  for the Faraday tensor,  $\star F^{\mu\nu}$  for the dual

<sup>\*</sup> E-mail: jmckinney@cfa.harvard.edu

of the Faraday, and  $T^{\mu\nu}$  for the stress-energy tensor. The field angular frequency is  $\Omega_F \equiv F_{t\theta}/F_{r\phi} = F_{t\theta}/F_{\theta\phi}$ . The magnetic field can be written as  $B^i = {}^*F^{it}$ . The poloidal magnetospheric structure is defined by the  $\phi$ -component of the vector potential ( $A_\phi \equiv \Psi$ ). The current system is defined by the current density ( $\mathbf{J}$ ) and the polar enclosed current ( $B_\phi \equiv {}^*F_{\phi t}$ ). The electromagnetic luminosity is  $L \equiv -2\pi \int_\theta d\theta T_t^r r^2 \sin\theta$ . See Gammie et al. (2003); McKinney & Gammie (2004); McKinney (2005d) for details.

## 2 NEUTRON STAR MAGNETOSPHERE

Here the implementation details and the solution to the neutron star magnetosphere are discussed. It is most useful to the community if a similar model to that chosen by Komissarov (2005) is studied and compared. This will show that one can study pulsar magnetospheres in the force-free limit using time-dependent numerical models. Despite the unphysical parameters introduced by Komissarov (2005), our solutions are similar.

The only additional note is that we and they choose a solution with no surface currents on the stellar surface by our and their choice of relaxed boundary conditions. This corresponds to, e.g., a neutron star with a crust in shear equilibrium (see, e.g., Ruderman et al. 1998). Other boundary conditions may lead to other solutions.

### 2.1 Initial and Boundary Conditions

As in Komissarov (2005), the magnetic field is approximated as an aligned dipolar field and the space-time is approximated as Minkowski. The poloidal field at  $t = 0$  (and for all time for  $B^r$ ) is set to be the perfect dipole with

$$A_\phi = \frac{B_{\text{pole}}}{2r} R_\star^3 \sin^2 \theta = \frac{\mu}{r} \sin^2 \theta, \quad (1)$$

where the magnetic dipole moment is  $\mu = B_{\text{pole}} R_\star^3 / 2$  for a polar magnetic field strength  $B_{\text{pole}}$  and stellar radius  $R_\star$ .

As in Komissarov (2005), the initial conditions are arbitrarily chosen to have a velocity of  $v^i = 0$  and  $B^\phi = 0$ , and the preceding violent non-stationary evolution eventually relaxes to a steady-state solution. Thus, any solution found must be a stable solution. As in Komissarov (2005), the model is evolved for 55 light cylinder times.

A steady-state solution with no discontinuities or surface currents on the stellar surface is found by choosing boundary conditions determined by an analysis of the Grad-Shafranov equation (see, e.g., Bogovalov 1997; Beskin 1997). One is required to specify 2 constraints and to fix the magnetic field component perpendicular to the star. As in Komissarov (2005),  $E_\phi \equiv F_{t\phi} = 0$ ,  $\Omega_F = \Omega_\star$ , and  $B^r$  are fixed in time, where  $\Omega_\star$  is the stellar angular velocity. This assumes the particle acceleration gap is negligible, which is not generally true (see, e.g., Mestel & Shibata 1994). The velocity obeys the frozen-in conditions (see equation 46 in McKinney 2005d) in steady-state and axisymmetry.

Komissarov (2005) set the radius of the star to be  $R_\star = 0.1R_L$ , where  $R_L = c/\Omega_F = c/\Omega_\star$  is the light cylinder. For  $R_\star = 10$  km, this means they chose a spin period of  $\tau \approx 2.1$  ms or  $\Omega_\star \approx 0.0207c^3/GM$  for a neutron star with  $M = 1.44M_\odot$ . We choose a similar frequency

of  $\Omega_\star \approx 0.0216c^3/GM$  such that the light cylinder is at  $R_L = 46.3GM/c^3$ .

In practice,  $B^r$  and  $\Omega_F = \Omega_\star$  are fixed, while  $B^\theta$  and  $B_\phi$  are parabolically extrapolated into the neutron star surface from the computational domain. For a stationary, axisymmetric force-free solution, one can show that the field geometry completely determines the velocity (see equation 47 in McKinney 2005d). For *arbitrary* field components  $B^i$  this prescription for  $v^i$  *always* leads to a time-like velocity within the light ‘‘cylinders’’ (McKinney 2005d).

The polar axis boundary condition is such that the perpendicular fluxes vanish. The outer boundary condition is obtained by extrapolating the field into the boundary zones and setting the velocity as described above, although the outer boundary is chosen to be far away to avoid reflections back onto the solution. In the event that there is a flux from the outer boundary into the computational grid, that flux is set to zero.

### 2.2 Coordinates

The computation is performed on a set of uniform rectangular coordinates described by the vector field  $x^{(\mu)}$ , where each uniform coordinate is arbitrarily mapped to, e.g.,  $t, r, \theta, \phi$  in spherical polar coordinates. Apart from the code’s ability to avoid significant numerical reconnection, the ability to choose an arbitrary  $\theta$  grid is crucial to obtain an accurate solution around the equatorial current sheet.

The radial coordinate is chosen to be

$$r = R_0 + e^{x^{(1)}}, \quad (2)$$

where  $R_0$  is chosen to concentrate the grid zones toward the surface (as  $R_0$  is increased from 0 to  $R_\star$ ). An inner radius of  $R_{in} = R_\star$ , an outer radius of  $R_{out} = 2315GM/c^2$  (50 light cylinders as in Komissarov 2005), and  $R_0 = 0.903R_\star$  are used.

The  $\theta$  coordinate is chosen to be

$$\theta = \pi x^{(2)} + \frac{1}{2}(1 - h(r)) \sin(2\pi x^{(2)}), \quad (3)$$

where  $x^{(2)}$  labels an arbitrary uniform coordinate and  $h(r)$  is used to concentrate grid zones toward or away from the equator. The wide dead zone in inner-radial regions and the current sheet in outer-radial regions are both resolved using

$$h(r) = \left( \frac{1}{2} + \frac{1}{\pi} \text{atan} \left( \frac{r - r_s}{r_0} \right) \right) (h_{\text{outer}} - h_{\text{inner}}) + h_{\text{inner}}, \quad (4)$$

where  $h_{\text{inner}} = 1.8$ ,  $h_{\text{outer}} = 0.05h_{\text{inner}}$ ,  $r_0 = 5GM/c^2$ , and  $r_s = 15GM/c^2$ .

Different resolutions were chosen to test convergence. In terms of radial vs.  $\theta$  resolution, we used  $64 \times 64$ ,  $80 \times 64$ ,  $80 \times 128$ ,  $80 \times 256$ ,  $80 \times 128$ ,  $160 \times 128$ ,  $160 \times 256$ , and finally for the fiducial model we used  $480 \times 256$  to reach a similar resolution of Komissarov (2005), who used  $496 \times 244$  for their final resolution. We find that all quantities have converged to within 1 – 5% at our highest resolution, where the exact percentage depends on the quantity.

### 2.3 Magnetosphere Solution

First, the code is checked that the solution reaches a steady-state. The solution does reach a well-defined steady-state by

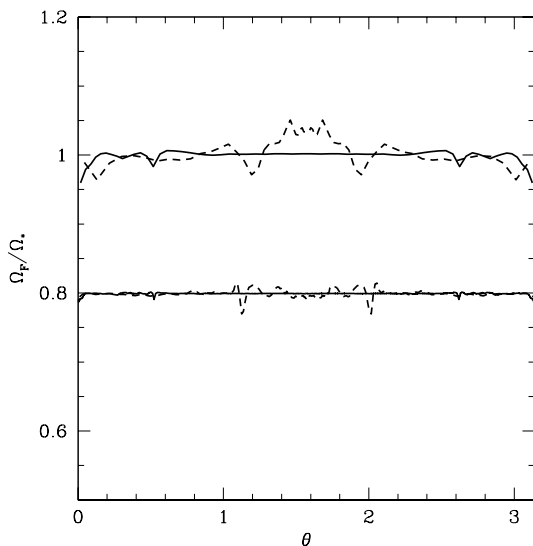


**Figure 1.** Upper two lines show the value of  $\Omega_F/\Omega_*$  as a function of  $\theta$  for  $r = 0.2R_L$  (solid line) and  $r = 0.7R_L$  (dashed line) for 64  $\theta$  zones and 80 radial zones. Lower lines show  $\Omega_F/\Omega_* - 0.2$  for 256  $\theta$  zones and 480 radial zones. Directly comparable to lower panels in figure 6 of Komissarov (2005).

about  $t \sim 1000GM/c^3$ , or after about 20 light cylinder light crossing times, out to about  $r \sim 1000GM/c^3$  for all of the domain except within the equatorial current sheet. The part of the equatorial current sheet that connects to the closed zone undergoes slow, small-amplitude oscillations. The frequency of these oscillations is proportional to the reconnection rate allowed by our reconnection model, while the amplitude is inversely proportional to the reconnection rate. Based upon the timing of the oscillations, the fiducial model has a reconnection period of  $\sim 10$ ms near the light cylinder. In the limit of an unlimited reconnection rate, there are no oscillations and the magnetosphere has a larger closed zone that extends somewhat beyond the light cylinder, similar to Komissarov (2005).

Second, the code is checked for proper integration. Since the neutron star has  $\Omega_* = \Omega_F$  over the entire surface, then in axisymmetry and for a stationary flow,  $\Omega_F$  should be the same for all field lines unless force-free (or ideal MHD) is violated. Notice that strong super-corotation (sub-corotation) would artificially enhance (diminish) the spindown luminosity and decrease (increase) the size of the closed zone. Figure 1 shows  $\Omega_F/\Omega_*$  as a function of  $\theta$  for  $r = 0.2R_L$  and  $r = 0.7R_L$ , the same locations as in Komissarov (2005) for their figure 6 (lower 2 panels). The plot is for  $t = 2546.3GM/c^3 \approx 55R_L/c$  for a  $\theta$  resolution of only 64 zones and 80 radial zones (upper lines) and of 256  $\theta$  zones by 480 radial zones (lower 2 lines displaced by 0.2). Komissarov (2005)’s figure shows that even at a  $\theta$  resolution of 244 that the peak-to-peak fractional variation is 22% near the equator and 45% overall (they have problems at the poles). Our model with only a  $\theta$  resolution of 64 has a peak-to-peak variation of only  $< 10\%$ , and there are no significant artifacts at the poles. Over the entire domain, the spin of the magnetosphere deviates at worst by 5%. At a resolution of  $480 \times 256$ , the variation of  $\Omega_F/\Omega_*$  over the

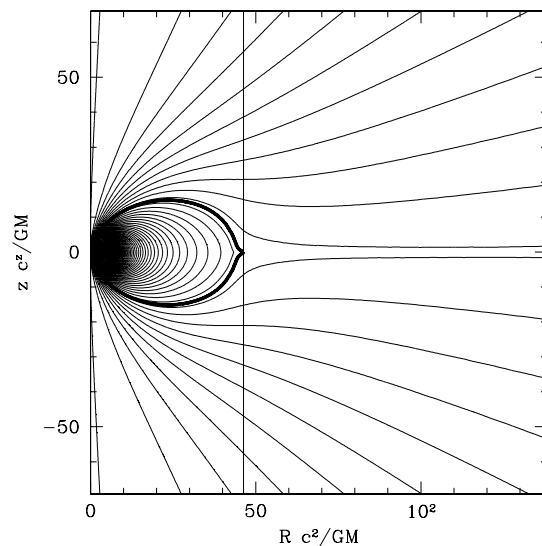


**Figure 2.** Flux function  $A_\phi$  in a box with size  $3R_L \times 3R_L$  ( $R_L$  is light cylinder) as in figure 3 (upper left panel) of Komissarov (2005). There are 80 contours from  $A_\phi = 0$  (polar axis) to  $A_\phi = \mu/R_* = 9.57\mu\Omega_*/c$  (equator on star). A single thick solid contour has been added for the closed field line that touches the theoretical light cylinder. The vertical solid line is the theoretical light cylinder  $R_L$ .

computational grid out to  $r \sim 1000GM/c^3$  (large radii still has initial transients) is  $< 3\%$ .

Finally, the region where the stationary solution is actually force-free is checked, which is tracked by our code (McKinney 2005d). Force-free is only violated in the very thin current sheet and only in the sheet for  $r > 2.8R_L$ . Energy is not strictly conserved when force-free is violated, but the volume occupied by this region is negligible and so energy loss is negligible and does not affect the luminosity as a function of radius described below.

Figure 2 shows the magnetic flux function ( $A_\phi$ ). The theoretical light cylinder at  $R = R_L$  very closely follows the true outer light cylinder except in the very thin current sheet, where the light “cylinder” extends slightly radially outward by  $\approx 5\%R_L$ . This magnetospheric structure is similar to the force-free solution of Contopoulos et al. (1999) (although they have some kinks at the light cylinder) and the MHD solution of Komissarov (2005).

Figure 3 shows the structure of the magnetosphere near the slightly dissipative current sheet. In our solutions and the solutions of Komissarov (2005), there are always some very thin, extended closed field loops at the equator. Using our low-resistivity model that keeps the current sheet from reconnecting, the heights of these extended closed field loops are smaller for increasing resolution, which also more sharply defines what is qualitatively associated with the so-called y-point. For general dissipative applications, however, the location of the y-point is ill-defined and cannot be quantitatively determined. Notice that while Komissarov (2005) state that their closed zone reaches all the way to the light cylinder, it is clear from their plots and other statements they make that there is no well-defined closed-open transition, which is consistent with our results. However, one

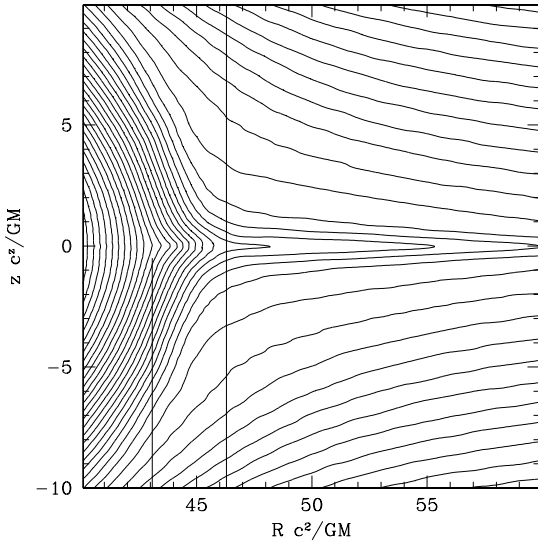


**Figure 3.** Flux function  $A_\phi$  for zoomed-in region of Figure 2 around light cylinder. There are 80 contours from  $A_\phi = 1.09\mu\Omega_\star/c$  to  $A_\phi = 1.80\mu\Omega_\star/c$ . The right vertical line represents the theoretical light cylinder. The left vertical line points to the field kink point at the equator.

can identify at least three quantitative measures, similar to Komissarov (2005).

First, the first closed field line to develop a kink at the equator near the light cylinder has an angle of

$$\theta_{\text{kink}} \approx 76^\circ \pm 3^\circ \quad (5)$$

between the field line and equator at the kink. This is similar to the solution found by Gruzinov (2005). As they found, we find that this result is independent of  $\Omega_\star$  since the solution is smooth through the surface. For the model being presented, the intersection of the kinked field line with the stellar surface is at  $\theta_{\text{kink},\star} \approx 70^\circ$  between a horizontal line and the field line at the stellar surface. The kink intersects the equator at

$$r_{\text{kink}} \approx 43.08 \pm 0.05 GM/c^2 = 0.931 \pm 0.001 R_L, \quad (6)$$

slightly within the theoretical light cylinder. The kink position oscillates in time by  $\approx \pm 0.01 R_L$ , where the prior error estimate is smaller since a mean position in time was isolated. At the kink, the vector potential has a value

$$A_\phi|_{\text{kink}} \equiv \Psi_{\text{kink}} = 1.35 \pm 0.01 \frac{\mu\Omega_\star}{c}, \quad (7)$$

which is quite close to the value of  $\Psi_{\text{open}} = 1.36\mu\Omega_\star/c$  given by Contopoulos et al. (1999) and by the value of  $\Psi_{yp} = 1.375 \pm 0.005\mu\Omega_\star/c$  given by Komissarov (2005). That the solution kinks before the theoretical light cylinder could be due to the lack of a perfect dipole due to the light cylinder being close to the stellar surface, the remaining dissipation in the model, or could be intrinsic to our stable model. A comparison of the numerical dissipative y-point and the theoretical dissipationless y-point (see, e.g., Uzdensky 2003) is left for future work.

The first kinked field line appears around  $r \approx 0.9 R_L$  in the fiducial model of Komissarov (2005), and this agrees

with our results. Since the nature of the dissipation is quite different in each code, this suggests that our similarly chosen  $\Omega_\star$  and so the lack of a perfect dipole, rather than dissipation, is the reason why the first kinked field line appears inside the theoretical light cylinder. Otherwise perhaps it is intrinsic to any stable solution.

Second, in Komissarov (2005) they *define* the “y-point” value of the vector potential to be at the theoretical light cylinder at  $\theta = \pi/2$ , which we find to be

$$A_\phi|_{R_L} \equiv \Psi_{\text{light}} = 1.27 \pm 0.01 \frac{\mu\Omega_\star}{c}, \quad (8)$$

which is quite close to the value of  $\Psi_{\text{separatrix}} \approx 1.27\mu\Omega_\star/c$  given by Gruzinov (2005), similar to  $\Psi_{\text{open}} = 1.23\mu\Omega_\star/c$  given in Contopoulos (2005), similar to  $\Psi_{\text{open}} = 1.27\mu\Omega_\star/c$  given by Timokhin (2005), and similar to  $\Psi_{\text{open}} = 1.265 \pm 0.005(\mu\Omega_\star/c)$  given by Komissarov (2005). Notice that the definition of the y-point value by Komissarov (2005) is their  $\Psi_{yp}$ , which we defined as  $\Psi_{\text{light}}$ . One should compare our  $\Psi_{\text{light}}$  to their  $\Psi_{yp}$ , which are the same measurement. However, while they get 1.37, we get 1.27 in units of  $c = \Omega_\star = \mu = 1$ .

Third, as in Komissarov (2005), the vector potential value continues to drop along the equator until  $r > 5R_L$  where their value just oscillates around  $\Psi_{\text{open}} \approx 1.265 \pm 0.005(\mu\Omega_\star/c)$ . We find that such a measurement gives

$$A_\phi|_{\text{open}} \equiv \Psi_{\text{open}} = 1.226 \pm 0.005 \frac{\mu\Omega_\star}{c}, \quad (9)$$

which is quite close to the value of  $\Psi_{\text{open}} = 1.23\mu\Omega_\star/c$  given in Contopoulos (2005) and slightly different than the value given by Komissarov (2005). That the value given by Komissarov (2005) is larger means they have more open flux. Thus, one expects their luminosity to be larger, which is the case.

Of significant interest is the luminosity coefficient of the dipolar approximation. We find that the luminosity is

$$L \approx 0.99 \pm 0.01 \frac{\mu^2 \Omega_\star^4}{c^3}. \quad (10)$$

This result for  $L$  agrees with the result by Gruzinov (2005), despite the detailed differences in the location of the kink-point, y-point, or the amount of open flux vs. closed flux. Since energy is explicitly conserved in our numerical method, the energy flux through each radius follows this same formula for the entire region that has reached a steady-state and does not violate force-free, unlike in Komissarov (2005) where energy is not explicitly conserved. Note that for a lower resolution model, e.g. 160 radial zones by 128  $\theta$  zones, that  $L \approx 1.10 \pm 0.05$  in units with  $\mu = \Omega_\star = c = 1$ , which is quite similar to the result by Komissarov (2005). Given that our code with 64  $\theta$  zones generated less error in  $\Omega_F$  than even their model with 244  $\theta$  zones, then likely their solution with  $496 \times 244$  radial vs.  $\theta$  zones is simply not as converged as our solution with  $480 \times 256$  zones. However, the agreement between our force-free model and their ideal MHD model is impressive given the many unphysical parameters they had to introduce to keep the solution realistic and the code stable (see their section 4.2).

Figure 4 shows the large-scale structure of the field at the final time of  $55R_L/c$  out to  $30R_L$ . There are 40 contours from  $A_\phi = 0$  to  $A_\phi = 1.41\mu\Omega_\star/c$ . The field is essentially monopolar. This is similar to Komissarov (2005), although a

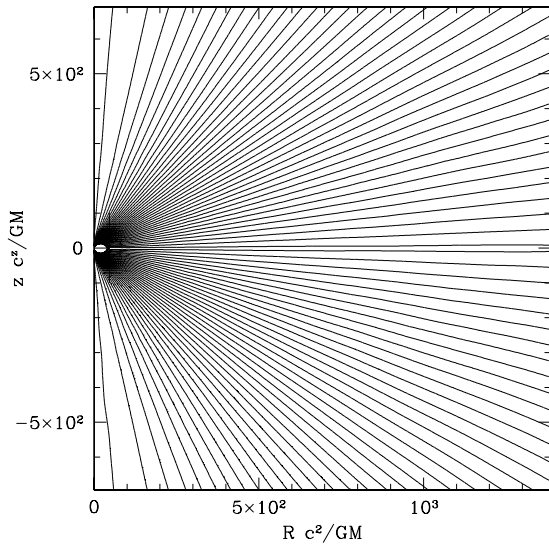


**Figure 4.** Flux function  $A_\phi$  out to  $30R_L$ . There are 40 contours from 0 to  $1.41\mu\Omega_*/c$ .

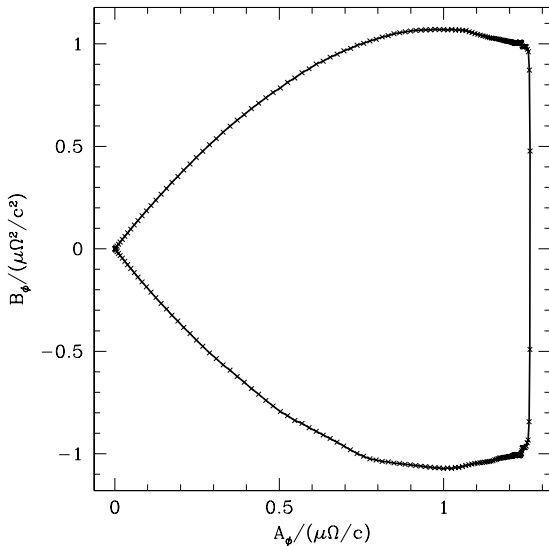


**Figure 5.** Current function  $B_\phi$  vs. flux function  $\Psi = A_\phi$ .

reconnection event and plasmoid motion disrupts their field at  $r \sim 23R_L$ .

A contour plot of the pulsar current function  $B_\phi$  shows that the quantity follows field lines and has a significant current increase across the separatrix. A plot of the current structure agrees with the classical model of pulsar current closure and with Komissarov (2005). To gain quantitative insight, Figure 5 shows the pulsar current function vs. the pulsar flux function, which is a similar plot to figure 4 in Komissarov (2005). We find that

$$\Psi_{\max} = 1.07 \frac{\mu\Omega_*}{c} \quad \text{at} \quad B_\phi = \pm 1.05 \frac{\mu\Omega_*^2}{c^2}, \quad (11)$$

at  $r = 1.1R_L$ . This is similar to the distribution shown by

Contopoulos et al. (1999) and is also similar to figure 4 in Komissarov (2005).

### 3 CONCLUSIONS

A stationary force-free solution is found for the neutron star magnetosphere with a dipolar surface field in Minkowski space-time with no stellar surface current. The luminosity follows the standard dipolar luminosity with a coefficient determined accurately to be  $k = 0.99 \pm 0.01$ .

The difficulties encountered by Komissarov (2005) in the force-free regime were avoided, and the unphysical parameters they introduced in the MHD regime were avoided. Their MHD solution is similar to our force-free solution, which suggests that the solution we and they find is accurate, stable, and may be unique.

### ACKNOWLEDGMENTS

This research was supported by NASA-Astrophysics Theory Program grant NAG5-10780 and a Harvard CfA Institute for Theory and Computation fellowship. I thank Serguei Komissarov and Dmitri Uzdensky for useful comments.

### REFERENCES

- Beskin, V. S. 1997, *Uspekhi Fizicheskikh Nauk*, 40, 659  
 Bogovalov, S. V. 1997, *A&A*, 323, 634  
 Contopoulos, I., Kazanas, D., & Fendt, C. 1999, *ApJ*, 511, 351  
 Contopoulos, I. 2005, *A&A*, 442, 579  
 Gammie, C. F., McKinney, J. C., & Gábor Tóth 2003, *ApJ*, 589, 444  
 Gammie, C. F., Shapiro, S. L., & McKinney, J. C. 2004, *ApJ*, 602, 312  
 Goldreich, P., & Julian, W. H. 1969, *ApJ*, 157, 869  
 Goodwin, S. P., Mestel, J., Mestel, L., & Wright, G. A. E. 2004, *MNRAS*, 349, 213  
 Gruzinov, A. 2005, *Physical Review Letters*, 94, 021101  
 Komissarov, S. S. 2002, *MNRAS*, 336, 759  
 Komissarov, S. S. 2004, *MNRAS*, 350, 427  
 Komissarov, S. S. 2005, *ArXiv Astrophysics e-prints*, arXiv:astro-ph/0510310  
 McKinney, J. C., & Gammie, C. F. 2004, *ApJ*, 611, 977  
 McKinney, J. C. 2005a, *ApJ*, 630, L5  
 McKinney, J. C. 2005b, *ArXiv Astrophysics e-prints*, arXiv:astro-ph/0506369  
 McKinney, J. C. 2005c, *ArXiv Astrophysics e-prints*, arXiv:astro-ph/0506368  
 McKinney, J. C. 2005d, *ArXiv Astrophysics e-prints*, arXiv:astro-ph/0601410  
 Mestel, L., & Shibata, S. 1994, *MNRAS*, 271, 621  
 Misner, C. W., Thorne, K. S., & Wheeler, J. A. 1973, *San Francisco: W.H. Freeman and Co.*, 1973,  
 Ruderman, M., Zhu, T., & Chen, K. 1998, *ApJ*, 492, 267  
 Ruderman, M. A., & Sutherland, P. G. 1975, *ApJ*, 196, 51  
 Timokhin, A. 2005, *ArXiv Astrophysics e-prints*, arXiv:astro-ph/0507054  
 Uzdensky, D. A. 2003, *ApJ*, 598, 446